*Astronomy & Astrophysics* manuscript no. article
November 19, 2015
© ESO 2015

arXiv:1511.05621v1 [astro-ph.HE] 17 Nov 2015

# Origin of the long-term modulation of radio emission of LS I +61°303

M. Massi[1] and G. Torricelli-Ciamponi[2]

[1] Max-Planck-Institut für Radioastronomie, Auf dem Hügel 69, D-53121 Bonn, Germany
e-mail: mmassi@mpifr-bonn.mpg.de
[2] INAF - Osservatorio Astrofisico di Arcetri, L.go E. Fermi 5, Firenze, Italy
e-mail: torricel@arcetri.astro.it

**ABSTRACT**

*Context.* One of the most unusual aspects of the X-ray binary LS I +61°303 is that at each orbit ($P_1$ = 26.4960 ± 0.0028 d) one radio outburst occurs whose amplitude is modulated with $P_{\rm long}$, a long-term period of more than 4 yr. It is still not clear whether the compact object of the system or the companion Be star is responsible for the long-term modulation.
*Aims.* We study here the stability of $P_{\rm long}$. Such a stability is expected if $P_{\rm long}$ is due to periodic ($P_2$) Doppler boosting of periodic ($P_1$) ejections from the accreting compact object of the system. On the contrary it is not expected if $P_{\rm long}$ is related to variations in the mass loss of the companion Be star.
*Methods.* We built a database of 36.8 yr of radio observations of LS I +61°303 covering more than 8 long-term cycles. We performed timing and correlation analysis. We also compared the results of the analyses with the theoretical predictions for a synchrotron emitting precessing ($P_2$) jet periodically ($P_1$) refilled with relativistic electrons.
*Results.* In addition to the two dominant features at $P_1$ and $P_2$, the timing analysis gives a feature at $P_{\rm long}$ = 1628 ± 48 days. The determined value of $P_{\rm long}$ agrees with the beat of the two dominant features, i.e. $P_{\rm beat} = 1/(\nu_1 - \nu_2)$ = 1626 ± 68 d. Lomb-Scargle results of radio data and model data compare very well. The correlation coefficient of the radio data oscillates at multiples of $P_{\rm beat}$, as does the correlation coefficient of the model data.
*Conclusions.* Cycles in varying Be stars change in length and disappear after 2-3 cycles following the well-studied case of the binary system $\zeta$ Tau. On the contrary, in LS I +61°303 the long-term period is quite stable and repeats itself over the available 8 cycles. The long-term modulation in LS I +61°303 accurately reflects the beat of periodical Doppler boosting (induced by precession) with the periodicity of the ejecta. The peak of the long-term modulation occurs at the coincidence of the maximum number of ejected particles with the maximum Doppler boosting of their emission; this coincidence occurs every $\frac{1}{\nu_1-\nu_2}$ and creates the long-term modulation observed in LS I +61°303.

**Key words.** Radio continuum: stars - Stars: jets - Galaxies: jets - X-rays: binaries - X-rays: individual (LS I +61°303 ) - Gamma-rays: stars

## 1. Introduction

The system LS I +61°303, which has an orbital period $P_1$ = 26.4960 ± 0.0028 days (Gregory 2002), is composed of a compact object and a massive star; the star has an optical spectrum typical of a rapidly rotating B0 V star with a decretion disc (Casares et al. 2005). At each orbit one radio outburst occurs whose amplitude is modulated with a long-term period $P_{\rm long}$ of 1605−1667 d (Marti & Paredes 1995; Gregory 2002). In this paper we study the origin of the long-term modulation. If it is attributable to periodic Doppler boosting effects, due to the precession of a jet associated with the compact object (Massi & Torricelli-Ciamponi 2014), then the long-term modulation has a stable periodicity. If it is attributable to an identical variation in the mass loss of the Be star (Gregory & Neish 2002), then the long-term modulation is rather unstable as it is in variable Be stars (Rivinius et al. 2013).

After examining the relationship between the long-term modulation and the period of the radio outburst (Sect. 2), we describe the precessing model (Sect. 3) and cyclic variability in Be stars (Sect. 4). In Sect. 5 we perform a timing and a correlation analysis on a radio data base of 36.8 yr, that covers more than 8 cycles of the long-term modulation. Finally, in Sect. 6 we discuss the implications of our results.

## 2. Relationship between the long-term modulation and the period of the radio outburst

In this section we analyse the relationship between the long-term period $P_{\rm long}$ and the radio outburst period $P_{\rm average}$. Their relationship, as shown below, is their mutual connection to the intrinsic periodicities of the system LS I +61°303, i.e. to the orbital period $P_1$ and to the precession $P_2$ of the jet.

### 2.1. Period of radio outbursts $P_{\rm average}$

The long-term periodicity $P_{\rm long}$ in LS I +61°303 is a phenomenon affecting not only the amplitude of the radio outburst, but also its position along the orbit (Paredes et al. 1990; Gregory 1999, 2002). The variation in the position of the outburst along the orbit, i.e. the orbital phase shift, depends on the timing residual between the orbital period $P_1$ and the actual occurrence of the radio outburst. The radio outburst occurs nearly but not exactly at $P_1$. Gregory (1999) showed that when radio outbursts are predicted to occur with $P_1$ then there are timing residuals of up to several days that follow a sawtooth trend with period $P_{\rm long}$. The same phenomenon has been analysed in terms of orbital phase shift by Paredes et al. (1990). An example is given

in Fig. 1. The top panel shows one outburst before the maximum of the long-term modulation at 49418 MJD (red), one outburst during the maximum at 49980 MJD (black), and one outburst towards the minimum at 50594 MJD (blue). In Fig. 1-centre we plot the three outbursts as function of the orbital phase Φ,

$$\Phi(P_1) = \frac{(t - t_0)}{P_1} - int\left[\frac{(t - t_0)}{P_1}\right], \quad (1)$$

where $t_0$=43366.275 MJD (Gregory 2002). The figure shows that the first outburst peaks at phase $\Phi(P_1) \sim 0.5$, whereas the second outburst is shifted at $\Phi \sim 0.6$, and the third at $\Phi \sim 0.8$. As can be seen in both Fig. 1-top and centre, there is a variation in the amplitude of the outburst at the same time as the orbital phase shift. The period of the amplitude modulation and the period of the sawtooth function are the same (Gregory 1999, 2002), so clearly the origin of the two phenomena are also the same. Why is there an orbital phase shift? or better, Why is there a timing residual with respect to the orbital period $P_1$? A saw-tooth function in the residuals is indicative of a systematic error, otherwise residuals should be randomly distributed. An intuitive answer is that $P_1$ is not the periodicity of the radio outburst. The first group to notice that the radio outburst periodicity is not equal to the orbital periodicity is Ray et al. (1997). In 1997 they reported a period for the radio outburst of 26.69 ± 0.02 d and discuss how their best estimate of the period is significantly different ($9\sigma$) from the best previously published value of 26.496 ± 0.008 d (Taylor & Gregory 1984). Based on the analysis of 6.5 years of Green Bank Interferometer (GBI) radio data, the period of $P_{\rm average}$ = 26.704 ± 0.004 d for the radio outbursts in LS I +61°303 has been confirmed, and noise-limited timing residuals between radio outbursts and predicted outbursts at $P_{\rm average}$ have been determined (Jaron & Massi 2013). The bottom panel of Fig. 1 shows that the three outbursts at the three different epochs all occur at the same $\Phi(P_{\rm average})$. The reason why the outburst period is called $P_{\rm average}$ is explained in the following section.

### 2.2. Beat between $P_1$ and $P_2$

Another peculiarity of the radio emission from this system is the variability of its morphology. Radio images at high angular resolution show an elongated feature that changes from a double-sided to a one-sided morphology and that continuosly changes position angle as well. A precession period of 27–28 d was estimated by VLBA astrometry (Massi et al. 2012). The observed flux density ($S_o$) of a synchrotron source is the intrinsic flux density ($S_i$) times the Doppler boosting factor (DB), which depends on the ejection angle. A periodic change in ejection angle of a radio emitting source, because of precession, changes the Doppler factor periodically; as a consequence, a periodicity should be observed in the flux density. Timing analysis of GBI radio data has revealed two periods (Massi & Jaron 2013), the already known orbital period $P_1$ = 26.49 ± 0.07 d ($\nu_1$ = 0.03775 d$^{-1}$) and a new period $P_2$ = 26.92 ± 0.07 d ($\nu_2$ = 0.03715 d$^{-1}$) consistent with the precessional period of 27–28 d indicated by the VLBA astrometry (Massi et al. 2012). The orbital period can result in a timing analysis if there is a periodical variation in the intrinsic flux density ($S_i$). The hypothesis that the compact object in LS I +61°303, which accretes material from the Be wind, undergoes a periodical ($P_1$) increase in the accretion rate $\dot{M}$ at a particular orbital phase along an eccentric orbit has been suggested and developed by several authors (Taylor et al. 1992; Marti & Paredes 1995; Bosch-Ramon et al. 2006; Romero et al. 2007).

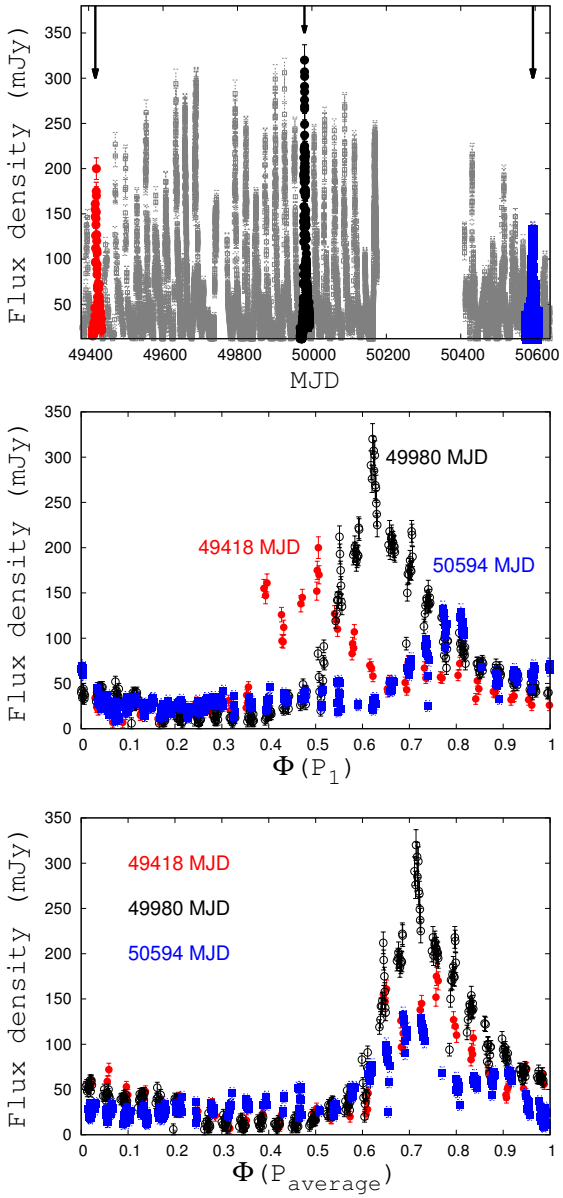


**Fig. 1.** Orbital phase shift in LS I +61°303. Top: consecutive radio outbursts in LS I +61°303. Three outbursts are indicated: one before the maximum of the long-term modulation, one at the maximum, one towards the minimum. Centre: the radio light curves are folded with the orbital phase $\Phi(P_1)$. The outburst does not follow the orbital periodicity and shifts at different epochs to different orbital phases. Bottom: the same light curves are here folded with $P_{\rm average}$, the periodicity of the radio outburst (Jaron & Massi 2013).

Recently, the presence of $P_1$ and $P_2$ have been confirmed as stable features in more recent Fermi-LAT and OVRO monitorings of the GeV gamma-ray emission (Jaron & Massi 2014) and of the radio emission (Massi et al. 2015), respectively.

The aim of the timing analysis was to obtain a better determination of the precessional period, but there was an additional and totally unexpected result: when combining $\nu_1$ and $\nu_2$ one obtains $P_{\rm average} = \frac{2}{\nu_1+\nu_2} = 26.70 \pm 0.05$ d and $P_{\rm beat} = \frac{1}{\nu_1-\nu_2} = 1667 \pm 393$ d (Massi & Jaron 2013). In other words, the beat of $P_1$ and $P_2$ creates $P_{\rm beat}$ (i.e. $P_{\rm long}$) that modulates their average $P_{\rm average}$. LS I +61°303 seems to be one more case in astronomy of a

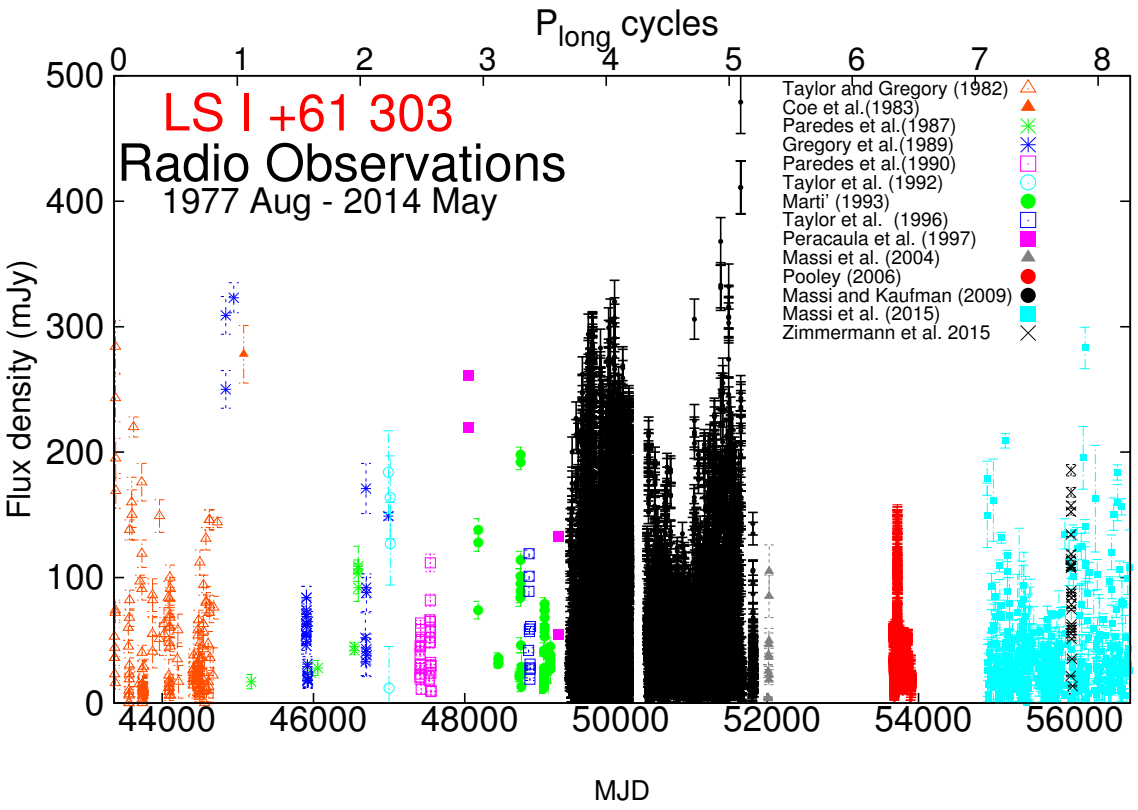


**Fig. 2.** Radio data of LS I +61°303 at 5, 8, 10, and 15 GHz from the literature. At the top x-axis are cycles of the long-term modulation, i.e. $t - t_0/1626$ (see Sect. 4). The archive covers more than 8 cycles.

"beat". The first astronomical case was a class of Cepheids, afterwards called Beat-Cepheids (Oosterhoff 1957). This phenomenon occurs when two physical processes create stable variations of nearly equal frequencies ($\nu_1$,$\nu_2$). The very small difference in frequency creates a long term variation ($\nu_1 - \nu_2$) modulating their average $(\nu_1 + \nu_2)/2$.

## 3. Precessing jet model

In our previous paper (Massi & Torricelli-Ciamponi 2014), we linked the two periodicities $P_1$ and $P_2$ to two physical processes: the periodic ($P_1$) increase of relativistic electrons in a conical jet due to $\dot{M}$ variations and the periodic ($P_2$) Doppler boosting of the emitted radiation by relativistic electrons due to jet precession. We have shown that the synchrotron emission of such a jet, calculated and fitted to the GBI observations, reproduces both the long-term modulation and the orbital phase shift of the radio outburst (Massi & Torricelli-Ciamponi 2014). The peak of the long-term modulation occurs when the jet electron density is around its maximum and the approaching jet forms the smallest possible angle with the line of sight. This coincidence of the maximum number of emitting particles and the maximum Doppler boosting of their emission occurs every $\frac{1}{\nu_1-\nu_2}$ and creates the long-term modulation observed in LS I +61°303. In this context, if no significant variations in $P_1$ and $P_2$ occur in the time interval under examination, then in that interval the long-term modulation remains stable.

## 4. Cyclic variability in the disc of some Be stars

The known long-term variability in Be stars is that of the violet-to-red cycles (V/R variations) in which the two peaks of the emission lines vary in height against each other. The variations correspond to an evolution of the disc itself where the disc undergoes a global one-armed oscillation instability that manifests itself in the V/R variability. This instability (progressing density wave) may eventually lead to the disruption of the disc, which after years or decades fills again (Grudzinska et al. 2015, and reference therein), and to cycle lengths that are not constant but vary from cycle to cycle (Rivinius et al. 2013, and references therein). We examine in detail the well-studied case of $\zeta$ Tau, which is also a Be star in a binary system. Over the last 100 years $\zeta$ Tau has gone through active stages characterized by pronounced long-term variations and quiet stages. From 1920 to about 1950 there were no variations. A very clear variability started afterwards and lasted until 1980 with 2 cycles of 2290 days and 1290 days. From 1980 to 1990 the star was again stable. Around 1990 the disc again entered into an active stage and 3 consecutive cycles of 1419 d, 1527 d, and 1230 d were determined (Štefl et al. 2009, and references therein). In this context, radio variations induced by variations in the Be disc are predicted to be rather unstable, i.e. to have cycles of different lengths and, at some epochs, to disappear.

## 5. Radio data base of LS I +61°303

We collected data of LS I +61°303 from the literature at 5, 8, 10, and 15 GHz (see Appendix) covering the interval 43367 MJD – 56795 MJD, i.e. 36.8 yr. To date, this is the largest archive on LS I +61°303. The data are shown in Figure 2. The top x-axis shows the number of cycles for a long-term period of 1626 d (see below): the data set covers 8 long-term cycles. In Fig. 3 we show the data overlapped with our physical model of the precessing jet assuming the same sampling and $\nu$ = 8 GHz. Our model was

fitted previously (Massi & Torricelli-Ciamponi 2014) on 6.7 yr of radio data (49380 MJD - 51823 MJD). As we show in Fig. 3, the model also reproduces well 36.8 yr of data.

In order to search for possible periodicities we used the Lomb-Scargle method, which is very efficient on irregularly sampled data (Lomb 1976; Scargle 1982). We use the algorithms of the UK Starlink software package, PERIOD (`http://www.starlink.rl.ac.uk/`). The statistical significance of a period is calculated in PERIOD following the method of Fisher randomization as outlined in Linnel Nemec & Nemec (1985). One thousand randomized time series are formed and the periodograms are calculated. The proportion of permutations in a given frequency window that give a peak power higher than that of the original time series provides an estimate of $p$, the probability that there is no such periodic component. A derived period is considered significant for $p < 0.01$ and marginally significant for $0.01 < p < 0.10$ (Linnel Nemec & Nemec 1985).

The spectrum is shown in Fig.4. We have two dominant features at $P_1 = 26.496 \pm 0.013$ d and $P_2 = 26.935 \pm 0.013$ d, evident in the zoom in the upper right panel. Period $P_1$ coincides with the orbital period (Gregory 2002) and period $P_2$ with the precession period (Massi & Jaron 2013; Massi et al. 2015). In the spectrum there is a third feature at $P_{\rm long} = 1628 \pm 49$ d. For all periods the randomization test gives $0.00 < p < 0.01$. It is interesting to compare this spectrum with that of the model shown in Fig. 4-right. Periods $P_1$, $P_2$, and $P_{\rm long}$ are all there. Period $P_{\rm long}$ shows two side lobes at 1265 d and at 2335 d; the small feature to the right of $P_{\rm long}$ in Fig. 4-left corresponds to 2335 d.

By comparing the light curves in Fig. 3 and the spectra, i.e. Fig. 4-left with Fig. 4-right, it is clear that the precessing jet model able to reproduce the light curve of 36.8 yr of radio data of LS I +61°303 also reproduces well its Lomb-Scargle spectrum. The most important result from the analysis of the largest archive of data available until now on LS I +61°303 is that it is evident for the first time that $P_{\rm long}$ is not a main characteristic of the Lomb-Scargle spectrum; the main characteristics are $P_1$ and $P_2$. We can compute the beating of the found $P_1$ and $P_2$ and check how $P_{\rm beat}$ compares with $P_{\rm long}$. The result is $P_{\rm beat} = (P_1 P_2)/(P_2 - P_1) = 1626 \pm 68$ d, clearly in agreement with $P_{\rm long} = 1628 \pm 49$ d.

How stable is the found $P_{\rm long}$ over the 8 cycles? This is the fundamental question of this work. A powerful method for studying the stability of a periodic signal over time is its autocorrelation. If a period is stable the correlation coefficient should appear as an oscillatory sequence with peaks at multiples of that period. We first examine the correlation coefficient for model data. The result is shown in Fig. 5-right. In the Lomb-Scargle spectrum, $P_{\rm long}$– given by the beating of $P_1$ and $P_2$ – is a minor feature; however, it becomes apparent in the plot of the correlation coefficient. We draw lines at multiples of $P_{\rm beat} = 1626$. Since $P_1$ and $P_2$ are constant in our model, it is clear that the model predicts a stable repetition of their beating frequency. We now compare the correlation of model data with the correlation of the observations. The correlation coefficient is shown in Fig. 5-left. Except for a slight drop in the correlation in the first cycles, the correlation coefficient of LS I +61°303 observations compares well with the correlation coefficient of the model data. The small drop in correlation is likely attributable to the data at 5 GHz present in the first 3.7 cycles (see Appendix). The scattering of the correlation coefficient around cycle 6 is due to the lack of data around that cycle (see Fig. 2); scattering is also present in the correlation of model data (Fig. 5-right).

## 6. Discussion and conclusions

We built a radio archive of 36.8 yr for the source LS I +61°303 and performed timing and correlation analysis. Our conclusions are the following:

1. In the system LS I +61°303 a periodic radio outburst is observed of $P_{\rm average} = 26.704 \pm 0.004$ d modulated by a long-term period of $1628 \pm 49$ d. However, the Lomb-Scargle spectrum is dominated by two other periodicities, $P_1 = 26.496 \pm 0.013$ d and $P_2 = 26.935 \pm 0.013$ d, and the observed periodicities $P_{\rm average}$ and $P_{\rm long}$ are equal to the beat of $P_1$ and $P_2$.
2. Synchrotron emission from a precessing jet model, with precession period $P_2$, regularly (with period $P_1$) refilled with relativistic electrons, reproduces the observed 36.8 yr light curve of LS I +61°303 and also its Lomb-Scargle spectrum.
3. The correlation coefficient of the observations shows a regular oscillation, as does the correlation coefficient of the model data with peaks at multiple of $P_{\rm long}$.

The period $P_{\rm long} = 1628 \pm 49$ d is stable over 8 cycles. This is not what is expected from Be wind variations, which are rather unstable and change from cycle to cycle or even disappear. A stable $P_{\rm long}$ is what is expected for a beat of periods $P_1$ (orbital period) and $P_2$ (precession) with no significant variations during the 8 examined cycles. The peak of the long-term modulation occurs when the jet electron density is around its maximum and the approaching jet forms the smallest possible angle with the line of sight. This coincidence of the maximum number of emitting particles and the maximum Doppler boosting of their emission occurs every $\frac{1}{\nu_1 - \nu_2}$ and creates the long-term modulation observed in the radio emission of LS I +61°303.

Finally, periods $P_1$ and $P_2$ have also been determined in the Lomb-Scargle spectrum of gamma-ray emission at apastron of Fermi-LAT data (Jaron & Massi 2014). Moreover, Paredes-Fortuny et al. (2015) discovered that the orbital phase shift also affects the variations in the equivalent width (EW) of the H$\alpha$ emission line from LS I +61°303. The orbital phase shift (Sect. 2.1) suggests that $P_{\rm average}$ is the true period for the EW variations. The EW variations show a long-term modulation as well (Zamanov et al. 2013). The presence of both long-term period and $P_{\rm average}$, as well as the direct detection of $P_1$ and $P_2$, indicates therefore that the precessing jet also induces variations in EW(H$\alpha$) and gamma-ray emission.

*Acknowledgements.* We are grateful to Hovatta Talvikky for providing the OVRO data and to Guy Pooley for providing the Ryle data. We acknowledge several helpful discussions with Frederic Jaron and Jürgen Neidhöferr. We acknowledge Atsuo Okazaki for suggesting the case of the Be star $\zeta$ Tau. We would like to thank the anonymous referee for the helpful comments. The OVRO 40 m Telescope Monitoring Program is supported by NASA under awards NNX08AW31G and NNX11A043G, and by the NSF under awards AST-0808050 and AST-1109911. This research is based on observations with the 100 m telescope of the MPIfR (Max-Planck-Institut fr Radioastronomie) at Effelsberg. The Green Bank Interferometer is a facility of the National Science Foundation operated by the NRAO in support of NASA High Energy Astrophysics programs.

## References

Bosch-Ramon, V., Paredes, J. M., Romero, G. E., & Ribó, M. 2006, A&A, 459, L25
Casares, J., Ribas, I., Paredes, J. M., Martí, J., Allende Prieto, C. 2005, MNRAS, 360, 1105
Coe, M. J., Bowring, S. R., Court, A. J., Hall, C. J., & Stephen, J. B. 1983, MNRAS, 203, 791
Gregory, P. C., Xu, H.-J., Backhouse, C. J., & Reid, A. 1989, ApJ, 339, 1054

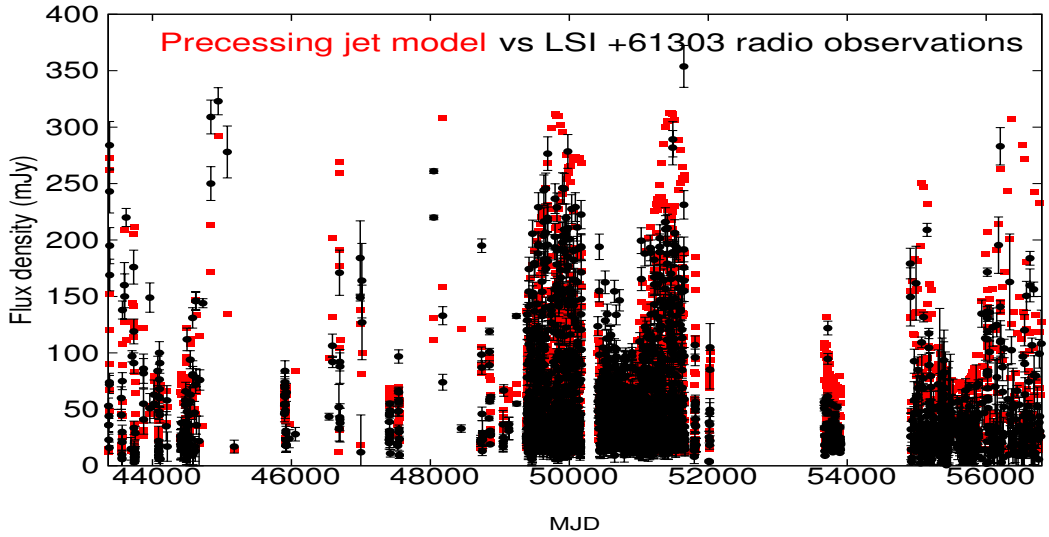


**Fig. 3.** Model data (red) and radio observations (black) of LS I +61°303 averaged over one day (Sect. 5).

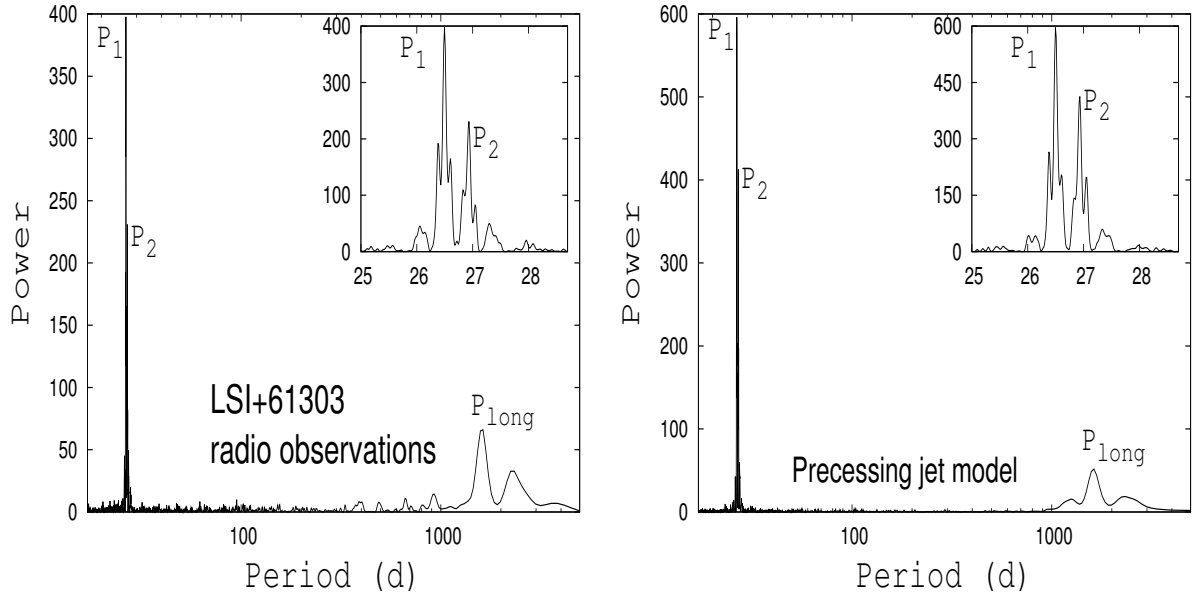


**Fig. 4.** Lomb-Scargle timing analysis of the observations (left) and the model data (right) of Fig. 3.

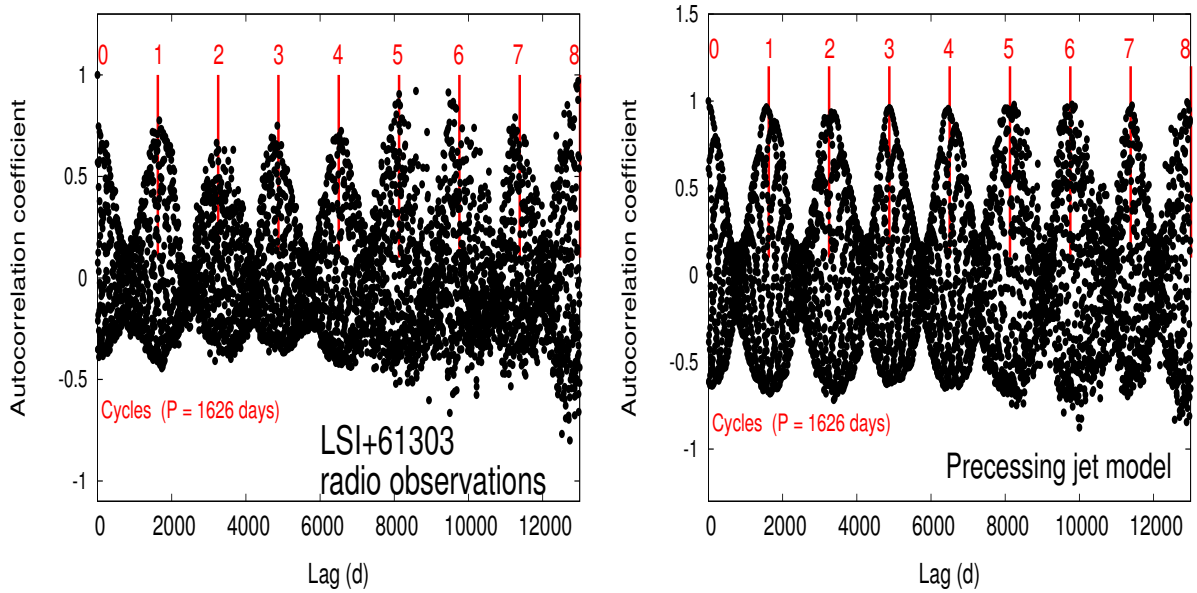


**Fig. 5.** Correlation coefficient vs time for observations (left) and model data (right), both averaged over three days.

Gregory, P. C. 1999, ApJ, 520, 361
Gregory, P. C. 2002, ApJ, 575, 427
Gregory, P. C., & Neish, C. 2002, ApJ, 580, 1133
Grudzinska, M., Belczynski, K., Casares, J., et al. 2015, MNRAS, 452, 2773
Jaron, F., & Massi, M. 2013, A&A, 559, A129
Jaron, F., & Massi, M., 2014, A&A, 572, A105
Linnell Nemec, A. F., & Nemec, J. M. 1985, AJ, 90, 2317
Lomb, N. R. 1976, Ap&SS, 39, 447
Martí, J. 1993, Ph.D. Thesis, University of Barcelona, "Radio emitting X-ray binaries"
Marti, J., & Paredes, J. M. 1995, A&A, 298, 151 A&A, 480, 289
Massi, M., Ribó, M, Paredes, J. M., et al. 2004, A&A, 414, L1
Massi, M., & Kaufman Bernadó, M. 2009, ApJ, 702, 1179
Massi, M., Jaron, F., & Hovatta, T. 2015, A&A, 575, L9
Massi, M., Ros, E., & Zimmermann, L. 2012, A&A, 540, A14
Massi, M., & Jaron, F. 2013, A&A, 554, A105
Massi, M., & Torricelli-Ciamponi, G. 2014, A&A, 564, AA23
Massi, M., Jaron, F., & Hovatta, T. 2015, A&A, 575, L9
Massi, M. 2014, Proceedings of the 12th European VLBI Network Symposium and Users Meeting (EVN 2014). 7-10 October 2014. Cagliari, Italy, PoS(EVN 2014)062.
Oosterhoff, P. T. 1957, Bulletin of the Astr. Inst. of the Netherlands, 13, 320
Paredes, J. M., Estalella, R., & Rius, A. 1987, A&A, 186, 177
Paredes, J. M., Estalella, R., Rius, A. 1990, A&A, 232, 377–380
Paredes-Fortuny, X., Ribó, M., Bosch-Ramon, V., et al. 2015, A&A, 575, L6
Peracaula, M., Marti, J., & Paredes, J. M. 1997, A&A, 328, 283
Pooley, G. G. 2006, VI Microquasar Workshop: Microquasars and Beyond, PoS(MQW6)019
Ray, P. S., Foster, R. S., Waltman, E. B., Tavani, M., & Ghigo, F. D. 1997, ApJ, 491, 381
Rivinius, T., Carciofi, A. C., & Martayan, C. 2013, A&A Rev., 21, 69
Romero, G. E., Okazaki, A. T., Orellana, M., & Owocki, S. P. 2007, A&A, 474, 15
Scargle, J. D. 1982, ApJ, 263,
Štefl, S., Rivinius, T., Carciofi, A. C., et al. 2009, A&A, 504, 929 835
Taylor, A. R., & Gregory, P. C. 1982, ApJ, 255, 210
Taylor, A. R., & Gregory, P. C. 1984, ApJ, 283, 273
Taylor, A. R., Kenny, H. T., Spencer, R. E., & Tzioumis, A. 1992, ApJ, 395, 268
Taylor, A. R., Young, G., Peracaula, M., Kenny, H. T., & Gregory, P. C. 1996, A&A, 305, 817
Zamanov, R., Stoyanov, K., Martí, J., et al. 2013, A&A, 559, A87
Zimmermann, L., Fuhrmann, L., & Massi, M. 2015, A&A, 580, L2

## Appendix A: Selection of frequencies for the radio data base

We selected from the literature data at 5, 8, 10, and 15 GHz. To reduce inhomogeneities in the archive, we excluded frequencies lower than 5 GHz because of the high flux that the 'second peak' can have at low frequency. The periodic radio outburst in LS I +61°303 is in fact not a simple, one-peak outburst. It may have a rather complex structure, mainly dominated by two consecutive peaks. These two peaks are 5-8 days apart and have different spectral characteristics; the first peak has a flat/inverted spectrum and the second outburst is optically thin, i.e. it dominates at low frequencies. At 8 GHz the second peak is often a minor peak, hardly traceable; instead, simultaneous observations at 2 GHz show a strong second peak, even larger at some epochs than the first peak (Massi & Kaufman Bernadó 2009; Massi 2014; Zimmermann et al. 2015).

We included data at 5 GHz to be able to cover the first cycles. However, at this frequency the second peak still seems to be significant and biases the correlation analysis slightly. The small drop in correlation coefficient from 1 to 0.7−0.8 (Fig.5-left) is likely attributable to the second peak at 5 GHz; for example in Table 1 in Taylor & Gregory (1982), a second peak of 91 ± 9mJy can be seen at 2444106.95 JD following the first peak (six days earlier) of 100 ± 10 mJy.